Matters arising

Zebrafish *prrx1a* mutants have normal hearts

Federico Tessadori[1], Dennis E. M. de Bakker[1,8], Lindsey Barske[2,6,7,8], Nellie Nelson[2], Hermine A. Algra[1], Sven Willekers[1], James T. Nichols[3], J. Gage Crump[2✉] & Jeroen Bakkers[1,4,5✉]

ARISING FROM O. H. Ocaña et al. *Nature* https://doi.org/10.1038/nature23454 (2017)

How organ laterality is established during embryo development is an intriguing question that remains largely unresolved. By using morpholino-based knockdown and CRISPR–Cas9-induced somatic mutations in zebrafish embryos, Ocaña et al.[1] reported a role for the paired-like homeobox transcription factor Prrx1a in a novel right-handed signalling pathway that drives cardiac looping. We analysed this process in two previously described frameshift *prrx1a*-mutant alleles[2], as well as in three newly generated large-deletion alleles that remove exon 1 and upstream sequences around the transcriptional start site (TSS), or the entire locus of the *prrx1a* gene such that no mRNA is produced. Homozygosity of any of these five alleles does not affect cardiac looping, which calls into question the requirement for *prrx1a* in left–right (L–R) patterning and cardiac development.

During embryogenesis, internal organs are laid out asymmetrically with respect to the embryonic midline. Laterality defects are relatively rare in humans, illustrating the robustness of the pathways that establish laterality. The initial break in L–R symmetry occurs at Kupffer's vesicle (a ciliated organ that directs L–R development) in zebrafish, Hensen's node in chick, and the node in mammalian embryos. The L–R information then propagates to the left lateral plate mesoderm (LPM) through asymmetric expression of the growth factor Nodal, resulting in the correct layout of the visceral organs, brain, heart and other structures[3]. On the basis of a transient right-biased expression of *prrx1a* in the LPM of zebrafish embryos, Ocaña et al.[1] used previously published splice-blocking and translation-blocking morpholino oligonucleotides (hereafter, morpholinos) against *prrx1a*[4] to inhibit its function, and reported defects in cardiac laterality in injected larvae. They also reported that zebrafish embryos injected with a single-guide RNA (sgRNA) and Cas9 protein inducing somatic *prrx1a* mutations displayed similar defects. Ocaña et al. concluded that *prrx1a* is an essential part of a right-handed signalling pathway that drives dextral heart looping[1].

We previously reported two germline frameshift mutant alleles for *prrx1a* that were generated with transcription activator-like effector nucleases (TALENs) (*prrx1a*[el558]) or with CRISPR–Cas9 (*prrx1a*[b1246])[2]. These alleles are predicted to abrogate the entire DNA-binding domain—similar to the expected effect of the splice-blocking morpholino (MO1) that was used by Ocaña et al.[1] (Fig. 1a, b). The *prrx1a*[el558] and *prrx1a*[b1246] alleles were found to result in no apparent morphological defects at any stage and to cause craniofacial defects only in combination with *prrx1b*-mutant alleles[2]. In contrast to the results of Ocaña et al. using morpholinos and sgRNA–Cas9 injection[1], we found that homozygous mutant embryos for *prrx1a*[el558] and *prrx1a*[b1246] showed a normal leftward

displacement of the linear heart tube (left cardiac jogging) at 26 hours post-fertilization (hpf), normal dextral heart looping at 50 hpf (Fig. 1d, e) and adult viability. Expression of *lefty2* (*lft2*) in the left LPM before the formation of the heart tube was also unaffected in *prrx1a*[el558] mutants (Fig. 1f). The lack of cardiac phenotypes was not due to compensation by the paralogue *prrx1b* or maternal supply of *prrx1a*, as cardiac looping was unaffected in *prrx1a*[el558/el558];*prrx1b*[el491/el491] double mutants (Fig. 1e) and in *prrx1a*[el558/el558] embryos obtained from homozygous mutant mothers (that is, maternal-zygotic knockouts, 40/40 left cardiac jogging).

Morpholinos and related antisense reagents have been widely used to inhibit gene function in many vertebrate organisms, including zebrafish, *Xenopus* and chick[5]. In some cases, however, morpholinos result in phenotypes that are not observed in corresponding homozygous loss-of-function zebrafish mutants—even when these were validated to result in a complete loss of functional protein[6,7]. These discrepancies have led to the introduction of community guidelines on the proper use of morpholinos[8], including obtaining similar phenotypes in the corresponding homozygous genetic null alleles when available, and showing that morpholinos do not cause additional phenotypes when injected into homozygous null mutants, particularly those that lack the morpholino target site. To test the specificity of the *prrx1a* splice-blocking MO1 (*prrx1a*-MO1) used by Ocaña et al.[1], we titrated and injected it into wild-type embryos and confirmed the reported effects on heart looping (Fig. 2a). However, we observed the same effects on heart looping when *prrx1a*-MO1 was injected into *prrx1a*[el558] zygotic mutant embryos, indicating that the observed laterality defects were probably not caused by knockdown of *prrx1a* (Fig. 2a). Similar results were obtained when *prrx1a*-MO1 was injected into *prrx1a*[el558/el558]; *prrx1b*[el491/el491] double mutants (Fig. 2a).

A number of explanations have been proposed for discrepancies between morpholino knockdown phenotypes and the lack thereof in germline mutants: off-target effects of morpholinos on splicing[9,10]; activation of the innate immune response by morpholinos[9]; production of functional proteins in mutants through alternate start codons, ribosomal frameshifting or alternate splicing[11]; and, most notably, upregulation of related genes in mutants (that is, 'transcriptional adaptation')[12]. Recent reports suggest that transcriptional adaptation is triggered by nonsense-mediated decay of mRNAs that encode proteins with premature stop codons[13,14]. We therefore generated three new *prrx1a* alleles that encompass large deletions that prevent the production of mRNAs. Two deletion mutants were made by deleting exon 1 and upstream sequences around the TSS (*prrx1a*[hu13685] and *prrx1a*[hu13762]; Fig. 1a). Quantitative PCR

[1]Hubrecht Institute–KNAW and University Medical Centre Utrecht, Utrecht, The Netherlands. [2]Department of Stem Cell Biology and Regenerative Medicine, Eli and Edythe Broad CIRM Center for Regenerative Medicine and Stem Cell Research, W. M. Keck School of Medicine, University of Southern California, Los Angeles, CA, USA. [3]Department of Craniofacial Biology, University of Colorado Anschutz Medical Campus, Aurora, CO, USA. [4]Department of Medical Physiology, Division of Heart and Lungs, University Medical Center Utrecht, Utrecht, The Netherlands. [5]Department of Pediatric Cardiology, Division of Pediatrics, University Medical Center Utrecht, Utrecht, The Netherlands. [6]Present address: Division of Human Genetics, Cincinnati Children's Hospital Medical Center, Cincinnati, OH, USA. [7]Present address: Department of Pediatrics, University of Cincinnati College of Medicine, Cincinnati, OH, USA. [8]These authors contributed equally: Dennis E. M. de Bakker, Lindsey Barske. ✉e-mail: gcrump@usc.edu; j.bakkers@hubrecht.eu
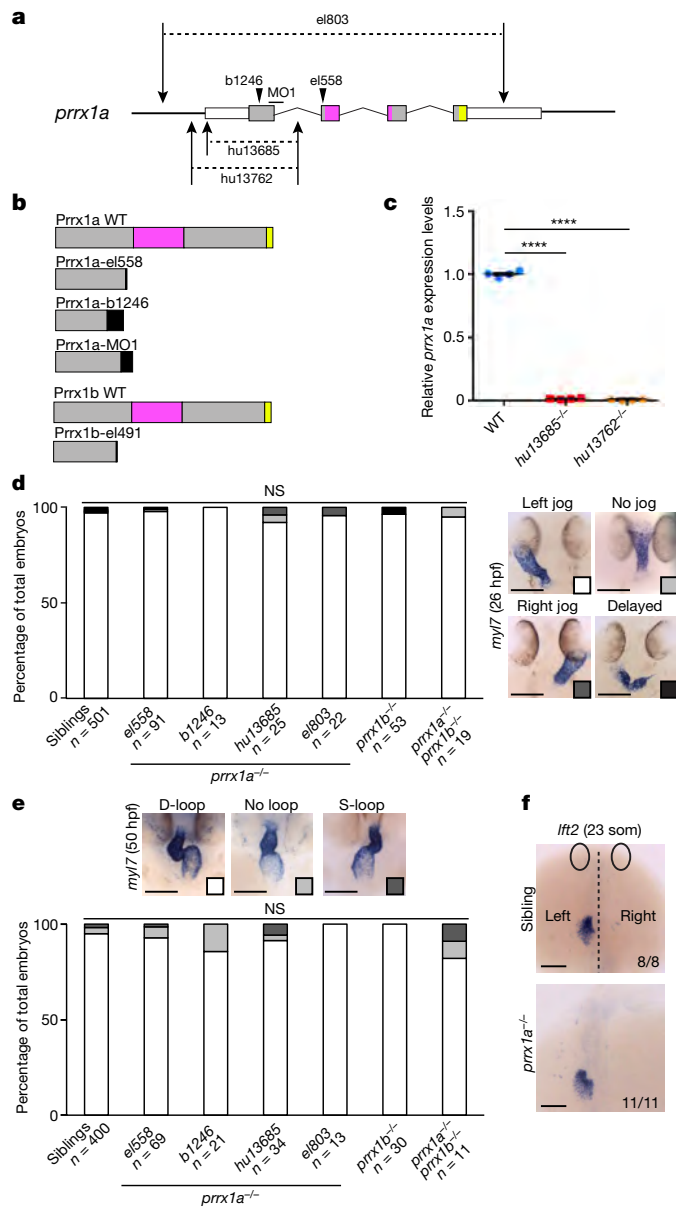
Fig. 1 | Cardiac laterality in *prrx1a*-mutant embryos. a, The *prrx1a* locus, genomic deletions (dashed lines) and sgRNA target sites (arrows). The horizontal bar indicates the MO1 target site. **b**, Predicted allelic *prrx1a*, *prrx1b* and *prrx1a*-MO1 translation products. In **a**, **b**, grey, coding regions; magenta, homeobox domain; yellow, OAR (otp/aristaless/rax) domain; black, aberrant additional amino acids. WT, wild type. **c**, Levels of *prrx1a* expression in *prrx1a^{hu13685/hu13685}* and *prrx1a^{hu13762/hu13762}* embryos (comparison to wild-type siblings). Two-tailed non-paired Student's *t*-test (****$P = 0.0001$); mean ± s.e.m. **d**, **e**, Cardiac phenotype of homozygous *prrx1a* mutants at 26 hpf (**d**) or 50 hpf (**e**) as scored by the cardiomyocyte marker *myl7* in situ hybridization or live imaging. D-loop, dextral loop; S-loop, sinistral loop. Chi-squared test: $\chi^2 = 20.03$, degrees of freedom (df) = 18, $P = 0.3309$ (**d**); $\chi^2 = 16.65$, df = 12, $P = 0.1634$ (**e**). NS, not significant. **f**, Expression of *lft2* at the 23-somite stage (23 som) is not affected in 11 out of 11 *prrx1a^{el558/el558}* embryos and 8 out of 8 wild-type siblings. Embryonic eyes are depicted as ovals. Statistical tests were carried out on entire datasets. No adjustments were made for multiple comparisons. For more details on statistics and reproducibility, see Supplementary Methods. Scale bars, 100 μm (**d**–**f**).

with reverse transcription (RT–qPCR) on RNA from single mutant or sibling embryos revealed that *prrx1a* mRNA was undetectable in homozygous mutant embryos of both lines (Fig. 1c). The third allele, *prrx1a^{el803}*, is a 7-kb deletion that encompasses the TSS and all exons, precluding
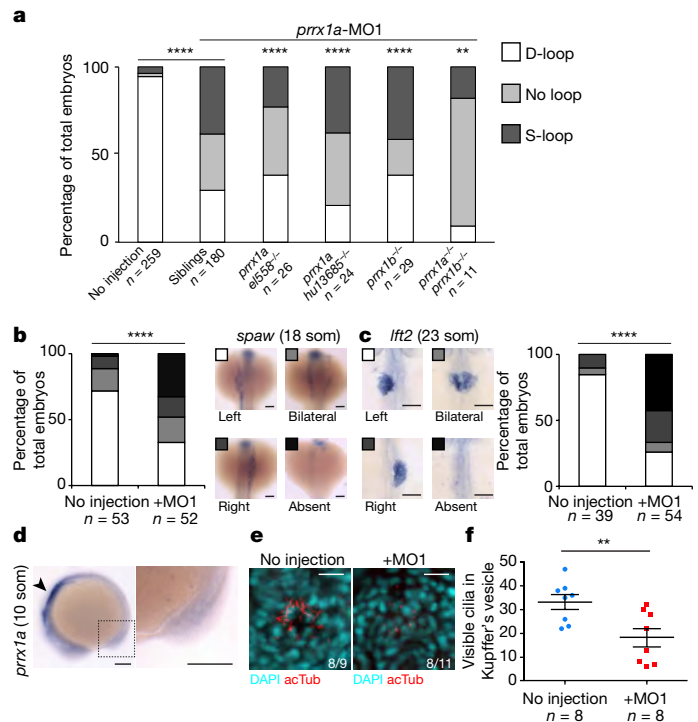

Fig. 2 | Induction of off-target laterality phenotypes by injection of *prrx1a*-MO1. The *prrx1a*-MO1 was injected at the same concentration (200 μM) as reported previously[1]. **a**, Cardiac-looping phenotypes of *prrx1a*-MO1-injected homozygous mutants and wild-type siblings at 50 hpf. Chi-squared test: no injection, siblings + MO1: $\chi^2 = 280.40$, df = 2, ****$P < 0.0001$; *el558^{-/-}*, *el558^{-/-}* + MO1: $\chi^2 = 32.81$, df = 2, ****$P < 0.0001$; *hu13685^{-/-}*, *hu13685^{-/-}* + MO1: $\chi^2 = 29.76$, df = 2, ****$P < 0.0001$; *prrx1b^{-/-}*, *prrx1b^{-/-}* + MO1: $\chi^2 = 26.80$, df = 2, ****$P < 0.0001$; *prrx1a^{-/-} prrx1b^{-/-}*, *prrx1a^{-/-} prrx1b^{-/-}* + MO1: $\chi^2 = 12.12$, df = 2, **$P = 0.0023$. Non-injected embryos of the corresponding genotype are taken as the non-injected control (Fig. 1e). **b**, **c**, Expression of *spaw* (18-somite stage) (**b**) and *lft2* (23-somite stage) (**c**) in *prrx1a*-MO1-injected wild-type embryos. Chi-squared test: no injection + MO1: $\chi^2 = 22.98$, df = 3, ****$P < 0.0001$ (**b**); no injection + MO1: $\chi^2 = 34.59$, df = 3, ****$P < 0.0001$ (**c**). **d**, In situ hybridization for *prrx1a* at the 10-somite stage (right, magnification of boxed region). Arrowhead indicates specific staining in the anterior LPM, which was observed in 28 out of 28 embryos. **e**, Representative projections of confocal stacks of Kupffer's vesicle in 12-somite-stage embryos stained with acetylated tubulin (acTub). Depicted phenotypes were observed in 8 out of 9 non-injected and 8 out of 11 *prrx1a*-MO1-injected embryos. **f**, Quantification of the number of cilia that stained positive for acetylated tubulin in **e**. Non-paired, two-tailed Student's *t*-test (**$P = 0.0092$); mean ± s.e.m. Statistical tests were carried out on entire datasets. No adjustments were made for multiple comparisons. For more details on statistics and reproducibility, see Supplementary Methods. Scale bars, 100 μm (**b**–**d**), 20 μm (**e**).

the production of mRNA and protein (Fig. 1a). Embryos homozygous for these large-deletion alleles exhibited normal cardiac jogging at 26 hpf and dextral heart looping at 50 hpf (Fig. 1d, e), and were viable. Analysis of these new deletion alleles therefore demonstrates that transcriptional adaptation mediated by mutant mRNA[13,14] cannot explain the discrepancy between the morpholino-induced phenotypes and the germline-mutant phenotypes. Furthermore, injection of *prrx1a*-MO1 into *prrx1a^{hu13685/hu13685}* mutants, which lack the target site for *prrx1a*-MO1, generated defects in cardiac looping, further confirming its lack of specificity (Fig. 2a).

To gain more insight into the possible cause of the morpholino-induced defects in heart looping, we analysed the expression of the Nodal-related *spaw* gene and *lft2*. Embryos injected with *prrx1a*-MO1 showed abnormal or absent expression of these left-sided genes (Fig. 2b, c). Furthermore, *prrx1a*-MO1-injected embryos exhibited a strong reduction in the number of cilia in the Kupffer's vesicle, and

Matters arising

prrx1a expression in this organ was below the level at which mRNA can be detected by in situ hybridization at this stage (Fig. 2d–f). Rather than disrupting dextral heart looping downstream of Nodal-related signalling, the *prrx1a*-MO1 appears to be acting earlier and non-specifically to alter the structure of Kupffer's vesicle.

In conclusion, we do not find a role for *prrx1a* in the establishment of a right-handed signalling pathway that drives heart looping in zebrafish. Our results demonstrate how a combination of frameshift alleles and larger-deletion alleles that do not produce mRNA should be used to resolve discrepancies between phenotypes that are observed in embryos with morpholino-induced knockdown and those observed in germline-mutant embryos. Whereas transcriptional adaptation can clearly explain the differences between knockdown and mutant phenotypes for some genes, in some cases—such as the heart-looping phenotypes analysed here—morpholinos produce non-specific effects that do not reflect endogenous gene function. Of note, gRNA–Cas9 reagents have also been reported to cause non-specific effects in injected zebrafish embryos[15], and we find that germline *prrx1a* mutants lack the cardiac-looping phenotypes that result from somatic CRISPR–Cas9 targeting of *prrx1a* as reported by Ocaña et al.[1]. On the other hand, morpholinos may still be of use in cases in which morpholinos and mutant alleles result in similar phenotypes—for example, the transient nature of morpholino-mediated knockdown can be taken advantage of to interfere with gene function only during embryogenesis. In summary, we suggest that great caution should be taken in interpreting phenotypes that are obtained by knockdown reagents, in particular in the absence of a priori knowledge of gene function, and that rigorous validation of phenotypes using both frameshift and larger transcript-less germline alleles that do not undergo transcriptional adaptation should be performed whenever possible.

Reporting summary

Further information on research design is available in the Nature Research Reporting Summary linked to this paper.

Data availability

All data are available within the manuscript and its associated files. Source data are provided with this paper.

1. Ocaña, O. H. et al. A right-handed signalling pathway drives heart looping in vertebrates. *Nature* **549**, 86–90 (2017).
2. Barske, L. et al. Competition between Jagged-Notch and Endothelin1 signaling selectively restricts cartilage formation in the zebrafish upper face. *PLoS Genet.* **12**, e1005967 (2016).
3. Blum, M., Feistel, K., Thumberger, T. & Schweickert, A. The evolution and conservation of left–right patterning mechanisms. *Development* **141**, 1603–1613 (2014).
4. Ocaña, O. H. et al. Metastatic colonization requires the repression of the epithelial-mesenchymal transition inducer Prrx1. *Cancer Cell* **22**, 709–724 (2012).
5. Heasman, J. Morpholino oligos: making sense of antisense? *Dev. Biol.* **243**, 209–214 (2002).
6. Kok, F. O. et al. Reverse genetic screening reveals poor correlation between morpholino-induced and mutant phenotypes in zebrafish. *Dev. Cell* **32**, 97–108 (2015).
7. Law, S. H. & Sargent, T. D. The serine-threonine protein kinase PAK4 is dispensable in zebrafish: identification of a morpholino-generated pseudophenotype. *PLoS One* **9**, e100268 (2014).
8. Stainier, D. Y. R. et al. Guidelines for morpholino use in zebrafish. *PLoS Genet.* **13**, e1007000 (2017).
9. Gentsch, G.E. et al. Innate immune response and off-target mis-splicing are common morpholino-induced side effects in *Xenopus*. *Dev. Cell* **44**, 597–610 (2018).
10. Joris, M. et al. Number of inadvertent RNA targets for morpholino knockdown in *Danio rerio* is largely underestimated: evidence from the study of Ser/Arg-rich splicing factors. *Nucleic Acids Res.* **45**, 9547–9557 (2017).
11. Anderson, J. L. et al. mRNA processing in mutant zebrafish lines generated by chemical and CRISPR-mediated mutagenesis produces unexpected transcripts that escape nonsense-mediated decay. *PLoS Genet.* **13**, e1007105 (2017).
12. Rossi, A. et al. Genetic compensation induced by deleterious mutations but not gene knockdowns. *Nature* **524**, 230–233 (2015).
13. El-Brolosy, M. A. et al. Genetic compensation triggered by mutant mRNA degradation. *Nature* **568**, 193–197 (2019).
14. Ma, Z. et al. PTC-bearing mRNA elicits a genetic compensation response via Upf3a and COMPASS components. *Nature* **568**, 259–263 (2019).
15. Hwang, W. Y. et al. Efficient genome editing in zebrafish using a CRISPR–Cas system. *Nat. Biotechnol.* **31**, 227–229 (2013).

Author contributions F.T.: project conception, experimental work, data analysis, manuscript writing; D.E.M.d.B.: project conception, experimental work; L.B.: experimental work, data analysis, manuscript revision; N.N.: experimental work, data analysis; H.A.A.: experimental work, data analysis; S.W.: experimental work; J.T.N.: zebrafish lines, manuscript revision; J.G.C.: zebrafish lines, project conception, manuscript writing; J.B.: project conception, manuscript writing.

Competing interests The authors declare no competing interests.

Additional information
Supplementary information is available for this paper at https://doi.org/10.1038/s41586-020-2674-1.
Correspondence and requests for materials should be addressed to J.G.C. or J.B.
Reprints and permissions information is available at http://www.nature.com/reprints.
Publisher's note Springer Nature remains neutral with regard to jurisdictional claims in published maps and institutional affiliations.

Corresponding author(s): Jeroen Bakkers

Last updated by author(s): Oct 25, 2019

Reporting Summary

Nature Research wishes to improve the reproducibility of the work that we publish. This form provides structure for consistency and transparency in reporting. For further information on Nature Research policies, see Authors & Referees and the Editorial Policy Checklist .

Statistics

For all statistical analyses, confirm that the following items are present in the figure legend, table legend, main text, or Methods section.

n/a	Confirmed	
	☒	The exact sample size (*n*) for each experimental group/condition, given as a discrete number and unit of measurement
	☒	A statement on whether measurements were taken from distinct samples or whether the same sample was measured repeatedly
	☒	The statistical test(s) used AND whether they are one- or two-sided *Only common tests should be described solely by name; describe more complex techniques in the Methods section.*
☒		A description of all covariates tested
☒		A description of any assumptions or corrections, such as tests of normality and adjustment for multiple comparisons
	☒	A full description of the statistical parameters including central tendency (e.g. means) or other basic estimates (e.g. regression coefficient) AND variation (e.g. standard deviation) or associated estimates of uncertainty (e.g. confidence intervals)
☒		For null hypothesis testing, the test statistic (e.g. *F*, *t*, *r*) with confidence intervals, effect sizes, degrees of freedom and *P* value noted *Give P values as exact values whenever suitable.*
☒		For Bayesian analysis, information on the choice of priors and Markov chain Monte Carlo settings
☒		For hierarchical and complex designs, identification of the appropriate level for tests and full reporting of outcomes
☒		Estimates of effect sizes (e.g. Cohen's *d*, Pearson's *r*), indicating how they were calculated

Our web collection on statistics for biologists contains articles on many of the points above.

Software and code

Policy information about availability of computer code

Data collection	Fig. 1d-f; Fig. 2b-d: Leica Application Suite LAS V4.3.0 Fig. 2e: Leica Application Suite LAS AF 2.7.4.10.100 For all above-mentioned figure panels, Adobe Photoshop CC2017 was used to make linear adjustments to whole pictures prior to composition of the figures in Adobe Illustrator CC2017.
Data analysis	Fig. 1c-e; Fig. 2a-c,f: GraphPad Prism 6.0c

For manuscripts utilizing custom algorithms or software that are central to the research but not yet described in published literature, software must be made available to editors/reviewers. We strongly encourage code deposition in a community repository (e.g. GitHub). See the Nature Research guidelines for submitting code & software for further information.

Data

Policy information about availability of data

All manuscripts must include a data availability statement. This statement should provide the following information, where applicable:

- Accession codes, unique identifiers, or web links for publicly available datasets
- A list of figures that have associated raw data
- A description of any restrictions on data availability

All data are available within the manuscript and its associated files. Source data behind Figures 1 and 2 are available within the manuscript files.

Field-specific reporting

Please select the one below that is the best fit for your research. If you are not sure, read the appropriate sections before making your selection.

☒

Life sciences study design

All studies must disclose on these points even when the disclosure is negative.

Sample size	Sample size was not predetermined statistically and is based on previous work in our laboratory.
Data exclusions	No exclusion criteria were used for analysis.
Replication	The experimental findings presented were reliably reproduced when applicable. For experiments carried out once, the number of zebrafish embryos analyzed ensures biological replication of the results.
Randomization	All analyzed embryos were chosen randomly.
Blinding	For all experiments reported in this study except the data presented in Fig.2b,c, scoring or quantification of the embryos was carried out blindly, ie the genotype of the embryos was determined only after completion of the scoring of all embryos. For data presented in Fig.2b,c the embryos used all have the same genotype (wild type) and the treatment used (no inj or MO1+) only affects embryos at the RNA level. Hence, it is not possible to determine the treatment undergone by the embryos a posteriori. Embryos pertaining to one or the other treatment hence had to be handled separately during the ISH protocol.

Reporting for specific materials, systems and methods

We require information from authors about some types of materials, experimental systems and methods used in many studies. Here, indicate whether each material, system or method listed is relevant to your study. If you are not sure if a list item applies to your research, read the appropriate section before selecting a response.

Materials & experimental systems

n/a	Involved in the study
☐	☒ Antibodies
☒	☐ Eukaryotic cell lines
☒	☐ Palaeontology
☐	☒ Animals and other organisms
☒	☐ Human research participants
☒	☐ Clinical data

Methods

n/a	Involved in the study
☒	☐ ChIP-seq
☒	☐ Flow cytometry
☒	☐ MRI-based neuroimaging

Antibodies

Antibodies used	Primary: mouse anti-acetylated tubulin monoclonal antibody (1:200; Sigma-Aldrich, Cat. T7451, Lot 086K435). Secondary: goat anti-mouse Cy3-conjugated secondary antibody (1:500; Jackson Immunoresearch, Cat. 115-165-146,)
Validation	Numerous publications on the manufacturer's website validate this antibody in various animal species. Sampaio et al., (PMID: 24930722) and Roxo-Rosa et al., 2015 (PMID: 26432887) use it specifically to label cilia in the zebrafish Kupffer's vesicle similarly to our study.

Animals and other organisms

Policy information about studies involving animals; ARRIVE guidelines recommended for reporting animal research

Laboratory animals	The zebrafish lines used in this study are Tübingen long fin (wild type), and prrx1ael558, prrx1ab1246, prrx1bel491; prrx1ael803, prrx1ahu13685 and prrx1ahu13762 . Age: Fig.1c: 2 days post fertilization (dpf); Fig.1d: 26 hours post fertilization (hpf); Fig.1e: 50 hpf; Fig.1f: 23 somites (approx. 20 hpf); Fig. 2a: 50 hpf; Fig. 2b: 18 somites (approx. 18 hpf); Fig. 2c: 23 somites (approx. 20 hpf); Fig. 1d: 10 somites (approx. 14 hpf), Fig. 1e: 12 somites (approx.
Wild animals	The study did not involve wild animals
Field-collected samples	The study did not involve data collected in the field
Ethics oversight	Animal experiments were approved by the Animal Experimentation Committee of the Royal Netherlands Academy of Arts and Sciences and the Institutional Animal Care and Use Committee of the University of Southern California.

Note that full information on the approval of the study protocol must also be provided in the manuscript.

Reply to: Zebrafish *prrx1a* mutants have normal hearts

Noemi Castroviejo[1], Oscar H. Ocaña[1,2], Luciano Rago[1,3], Hakan Coskun[1,4], Aida Arcas[1,5], Joan Galcerán[1] & M. Angela Nieto[1✉]

In our original paper we showed that left–right (L–R) asymmetric cell movements towards the midline produced differential forces that lead to a leftward displacement of the cardiac posterior pole, initiating heart laterality[1]. We also showed that the cell movements were mediated by the L–R asymmetric activation (higher on the right) of transcription factors (Snail and/or Prrx) that induce epithelial–mesenchymal transition (EMT), and that this cellular behaviour is conserved in zebrafish, chicken and mouse[1]. In the accompanying Comment, Tessadori et al.[2] question the role of Prrx1a in heart laterality in zebrafish, after generating mutants that do not present heart laterality defects. Injection of one of the morpholinos we used (MO1) into zygotic *prrx1a*[el558] and *prrx1a*[hu13685] mutant embryos led to a cardiac phenotype that was considered to result from off-target mediated effects that act early in development and alter the structure of the left–right organizer (LRO) (also known as Kupffer's vesicle) in zebrafish[3–5]. Thus, two questions arise. First, whether the mesocardia phenotype that we observed in *prrx1a*-MO1 embryos was due to non-specific off-target effects; and second, whether Prrx1a is dispensable for heart laterality in zebrafish. Here we provide new data indicating that Prrx1a has a role in heart laterality in zebrafish (Fig. 1).

We also show that although Prrx1a may be dispensable, as seen in genetic knockout experiments, other EMT transcription factors (namely Twist1a and Snail1b) are also expressed in a L–R asymmetric manner in the relevant region of the anterior lateral plate mesoderm (ALPM). Furthermore, G0 CRISPR-induced mutant (crispant) embryos for *twist1a* and *snail1b* also show mesocardia (Fig. 2), raising the possibility that they may cooperate with and/or compensate for the loss of Prrx1a and, if so, explaining the absence of cardiac laterality defects in *prrx1a* zebrafish mutants.

To further examine the specificity of the heart phenotype, we generated *prrx1a*-crispant embryos (G0) with an additional set of guides (Fig. 1a), and using a Cas9 protein optimized to prevent off-target function[6,7], in conditions that have been shown to generate mutagenized G0 embryos that lack confounding non-specific traits[6]. Prrx1a protein cannot be detected in these embryos, confirming the efficiency of the guides (Fig. 1b) and showing that mutations are induced in virtually all copies of the targeted gene in the zebrafish G0 crispant embryos[6]. These embryos show the same defects that we described previously[1]—namely mesocardia (although at a lower penetrance) and a reduction in the size of the atrium (Fig. 1c, d). Other defects, such as a smaller head, were also previously observed in *prrx1a* and *prrx1b* double mutants[8]. Notably, both the cilia in the LRO and the expression of *spaw* appear normal (Fig. 1e, f), indicating that the crispant embryos do not have the early defects in the LRO that were observed in the morpholino-induced

mutant embryos and that could non-specifically influence heart laterality. Moreover, the decision of the posterior pole of the heart to move from the midline to the left occurs late—independent of the formation of the LRO and heart jogging[9,10]. This is also in agreement with our photoablation experiments that were performed after jogging[1].

We generated a *prrx1a*-mutant allele (*prrx1a*[in69]) using the set of guides that was also used for the generation of crispant embryos (yellow in Fig. 1a, g). This mutant allele generates a *prrx1a* transcript that lacks the splice site at exon 1 and hence cannot encode a functional Prrx1a protein (Fig. 1g). Thus, the *in69* mutation is equivalent to a *prrx1a* loss-of-function mutation. This mutant—like the *prrx1a* null mutants *hu13685*, *hu13762* and *el803*—does not show mesocardia, indicating that Prrx1a may be dispensable, as suggested by Tessadori et al.[2]. However, this does not necessarily mean that Prrx1a is not involved in heart laterality. The *in69* mutant allows us to directly examine the specificity of the RNA guides in targeting *prrx1a*, as the corresponding guide sequences are not present in its genome. As expected for a bona fide specificity control, when *prrx1a*[in69] homozygous mutant embryos are injected with these guides they do not show any detectable defect, whereas the injection of these guides into wild-type sibling embryos leads to mesocardia (Fig. 1g). Thus, although we cannot formally exclude the existence of an off-target effect, all of this evidence supports that the mesocardia phenotype we observe in G0 crispant embryos is a specific effect of targeting the *prrx1a* gene.

Germline mutations might compensate for deficiencies that cannot be compensated after acute losses such as the somatic mutations induced by CRISPR–Cas9, with the latter revealing putative gene redundancy[6]. Compensatory mechanisms include transcriptional adaptation through mRNA nonsense-mediated decay[11,12] or activation of paralogues, but these mechanisms are rejected by Tessadori et al.[2]. Notably, compensation can also be achieved by non-paralogous genes, provided they have similar functions[13]. We have now found a transient L–R asymmetric expression pattern similar to that of *prrx1a* for two other EMT transcription factor genes—*snail1b* and *twist1a*—in the ALPM, in which the precursor cells of the second heart field are located (Fig. 2a). G0 crispant embryos for *snail1b* or *twist1a* also showed a heart laterality phenotype (Fig. 2b), and we have previously shown that Twist transcription factors can cooperate with Prrx1 in zebrafish and in cancer cells[14]. Thus, all of these data are compatible with a scenario in which the three EMT transcription factors cooperate in the regulation of heart laterality, and in which Snail1b and/or Twist1a might compensate for the loss of Prrx1a.

With respect to the mechanism we described for heart lateralization in vertebrates, we showed that a similar mechanism operates in the

[1]Instituto de Neurociencias (CSIC-UMH), Sant Joan d'Alacant, Alicante, Spain. [2]Present address: Centro Nacional de Investigaciones Cardiovasculares (CNIC), Madrid, Spain. [3]Present address: Department of Oncogenomics, Academic Medical Center, Amsterdam, The Netherlands. [4]Present address: Boston Children's Hospital, Harvard Medical School, Harvard University, Boston, MA, USA. [5]Present address: Centro de Investigación Médica Aplicada (CIMA), University of Navarra, Pamplona, Spain. ✉e-mail: anieto@umh.es
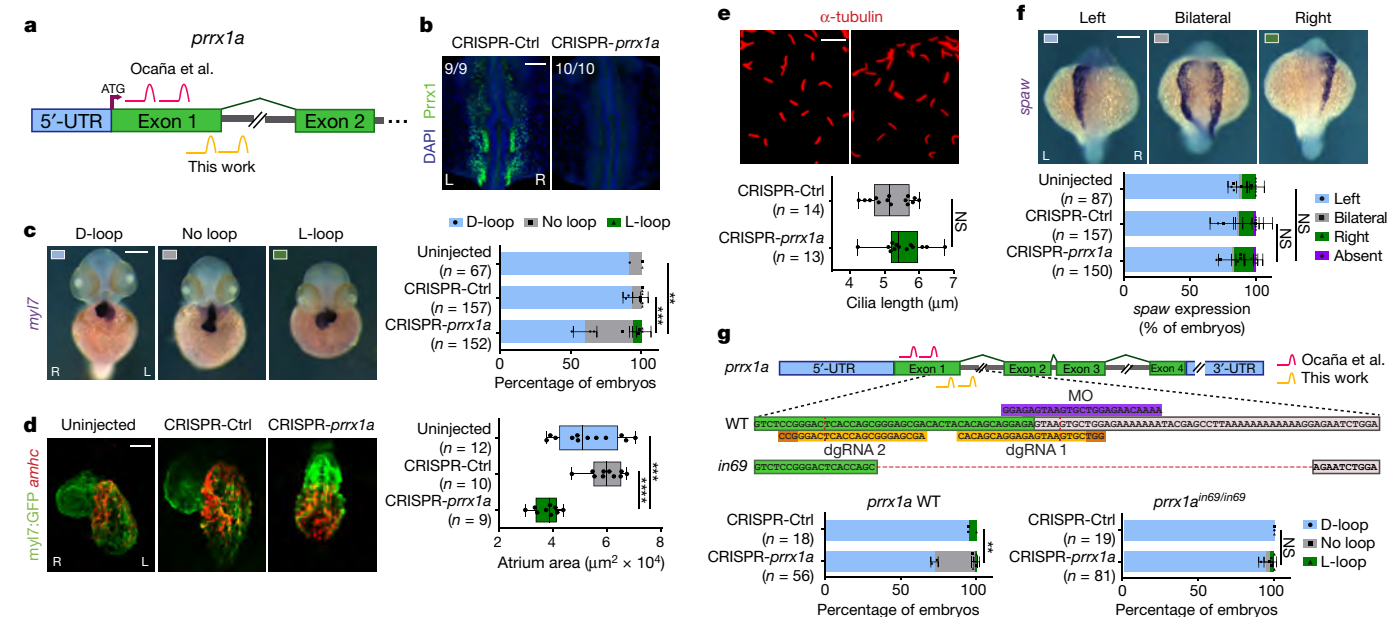
Matters arising

Fig. 1 | *prrx1a*-crispant embryos show mesocardia and a smaller atrium without early defects in the LRO. a, Schematic representation of the *prrx1a* gene and the RNA guides used previously[1] (pink) or in this work (yellow). UTR, untranslated region. **b**, Immunofluorescence at the 18-somite stage shows the absence of Prrx1a protein in *prrx1a*-crispant embryos (dorsal view). **c**, Analysis of heart position at 52 hours post-fertilization (hpf) shows mesocardia (no loop) in *prrx1a*-crispant embryos. Images are shown in ventral view. D-loop, posterior pole to the left and dextral loop; L-loop, posterior pole to the right and sinistral loop. **d**, Whole-mount in situ hybridization for *amhc* (atrial marker) in Tg(myl7:GFP) embryos (in which a *myl7* promoter drives GFP expression in cardiomyocytes) at 52 hpf. *prrx1a*-crispant embryos show a reduction in the size of the atrium. Images are shown in ventral view. **e**, Immunofluorescence of acetylated α-tubulin shows that cilia in the Kupffer's vesicle are not affected in 8-somite-stage *prrx1a*-crispant embryos. **f**, Normal left-sided *spaw* transcripts in 20-somite-stage *prrx1a*-crispant embryos (dorsal view). **g**, The *prrx1a* gene, with coding sequences highlighted in green and intron sequences in grey. The *prrx1a^in69* allele contains a 69-nucleotide deletion

generated using the new CRISPR-*prrx1a* guides (yellow). Protospacer adjacent motif (PAM) sequences are highlighted in orange and the predicted sites of Cas9 digestion are marked with red dotted lines. The *in69* allele lacks both of the guide sequences (yellow) at the *prrx1a* locus. The position of the morpholino (MO) in our original study[1] is highlighted in purple. As expected from the lack of the guide sequences in the mutant and for a bona fide specificity control, only the embryos with wild-type (WT) alleles present a mesocardia phenotype after injection of CRISPR–Cas9 *prrx1a* reagents. dgRNA, dual-guide RNA. Data in **c**, **f**, **g** are mean percentage ± s.d. In box plots (**d**, **e**), centre lines, medians; box limits, second and third quartiles; whiskers, first and fourth quartiles. *n* = number of embryos analysed from one (**d**, **e**), two (**b**, **g**) or three (**c**, **f**) independent experiments. Statistical analysis: two-way analysis of variance (ANOVA) (**c**, **f**, **g**); one-way ANOVA (**d**); unpaired Student's *t*-test (two-tailed) (**e**). NS, not significant, **P < 0.01, ***P < 0.001, ****P < 0.0001. Scale bars, 200 μm (**b**), 250 μm (**c**, **f**), 50 μm (**d**) and 40 μm (**e**). See Supplementary Methods.
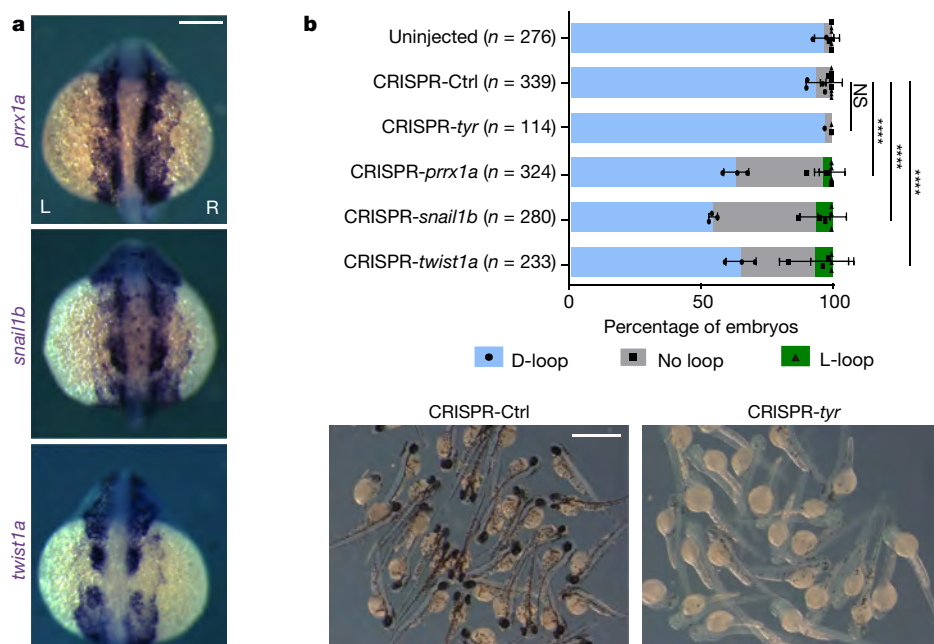

Fig. 2 | EMT transcription factors in heart laterality in zebrafish. a, L–R asymmetric expression of the EMT transcription factors *prrx1a, snail1b* and *twist1a* in the ALPM of 20-somite-stage embryos (dorsal view). Representative images from two independent experiments (total number of embryos, *n* = 60). **b**, Heart position at 52 hpf in crispant embryos for *prrx1a, snail1b, twist1a* and *tyr* (tyrosinase; negative control). Note the efficacy of editing in the zebrafish population, as assessed by the level of pigmentation. Data are mean percentage ± s.d. *n* = number of embryos analysed from one independent experiment (CRISPR-*tyr*) or three independent experiments (for each EMT transcription factor). Statistical analysis (shown for the mesocardia phenotype; grey): two-way ANOVA. NS, not significant, ****P < 0.0001. Scale bars, 250 μm (**a**) and 1.5 mm (**b**). See Supplementary Methods.

chick embryo (using short interfering RNA (siRNA)), and in the mouse embryo (using conditional mutants)[1]. Furthermore, this mechanism is compatible with previous studies that proposed a L–R asymmetric contribution to the posterior pole of the heart for heart laterality[15,16]. In addition, with regard to the conservation of the Nodal pathway in vertebrates[5], we have shown that the transient L–R asymmetric expression of EMT transcription factors that leads to differential L–R cell movements is established by a Nodal-mediated transient activation of microRNAs in the LPM. Deregulation of these microRNAs by gain and CRISPR–Cas9-mediated loss of function, or by genetic deletion of their binding sites in *Prrx1* or *Snail1* 3′ untranslated regions, led to bilateral symmetric expression of Prrx1 and Snail1 and mesocardia in both zebrafish and mice[17].

All of the data above, together with previous comprehensive morphological, functional and computational studies of cardiac development in mice[18,19], support our conclusion that the displacement of the posterior pole of the vertebrate heart from the midline implies a differential L–R EMT[1]. Whether other EMT transcription factors compensate for Prrx1a loss, and how the right-handed heart looping occurs after the leftward displacement of the posterior pole, deserve further investigation, although the latter is probably driven by intrinsic cues, as previously suggested[9,10].

Reporting summary

Further information on research design is available in the Nature Research Reporting Summary linked to this paper.

Data availability

All of the raw data that support the findings of this study are available within the manuscript and its associated files. Source data are provided with this paper.

1. Ocaña, O. H. et al. A right-handed signalling pathway drives heart looping in vertebrates. *Nature* **549**, 86–90 (2017).
2. Tessadori, F. et al. Zebrafish *prrx1a* mutants have normal hearts. *Nature* https://doi.org/10.1038/s41586-020-2674-1 (2020).
3. Collignon, J., Varlet, I. & Robertson, E. J. Relationship between asymmetric nodal expression and the direction of embryonic turning. *Nature* **381**, 155–158 (1996).
4. Long, S., Ahmad, N. & Rebagliati, M. The zebrafish *nodal*-related gene *southpaw* is required for visceral and diencephalic left-right asymmetry. *Development* **130**, 2303–2316 (2003).
5. Montague, T. G., Gagnon, J. A. & Schier, A. F. Conserved regulation of Nodal-mediated left–right patterning in zebrafish and mouse. *Development* **145**, dev171090 (2018).
6. Hoshijima, K. et al. Highly efficient CRISPR–Cas9-based methods for generating deletion mutations and F0 embryos that lack gene function in zebrafish. *Dev. Cell* **51**, 645–657 (2019).
7. Vakulskas, C. A. et al. A high-fidelity Cas9 mutant delivered as a ribonucleoprotein complex enables efficient gene editing in human hematopoietic stem and progenitor cells. *Nat. Med.* **24**, 1216–1224 (2018).
8. Barske, L. et al. Competition between Jagged-Notch and endothelin1 signaling selectively restricts cartilage formation in the zebrafish upper face. *PLoS Genet.* **12**, e1005967 (2016).
9. Noël, E. S. et al. A Nodal-independent and tissue-intrinsic mechanism controls heart-looping chirality. *Nat. Commun.* **4**, 2754 (2013).
10. Grimes, D. T. et al. Left-right asymmetric heart jogging increases the robustness of dextral heart looping in zebrafish. *Dev. Biol.* **459**, 79–86 (2020).
11. El-Brolosy, M. A. et al. Genetic compensation triggered by mutant mRNA degradation. *Nature* **568**, 193–197 (2019).
12. Ma, Z. et al. PTC-bearing mRNA elicits a genetic compensation response via Upf3a and COMPASS components. *Nature* **568**, 259–263 (2019).
13. Pasek, S., Risler, J. L. & Brézellec, P. The role of domain redundancy in genetic robustness against null mutations. *J. Mol. Biol.* **362**, 184–191 (2006).
14. Ocaña, O. H. et al. Metastatic colonization requires the repression of the epithelial–mesenchymal transition inducer Prrx1. *Cancer Cell* **22**, 709–724 (2012).
15. Taber, L. A., Voronov, D. A. & Ramasubramanian, A. The role of mechanical forces in the torsional component of cardiac looping. *Ann. NY Acad. Sci.* **1188**, 103–110 (2010).
16. Domínguez, J. N., Meilhac, S. M., Bland, Y. S., Buckingham, M. E. & Brown, N. A. Asymmetric fate of the posterior part of the second heart field results in unexpected left/right contributions to both poles of the heart. *Circ. Res.* **111**, 1323–1335 (2012).
17. Rago, L. et al. MicroRNAs establish the right-handed dominance of the heart laterality pathway in vertebrates. *Dev. Cell* **51**, 446–459 (2019).
18. Tautz, D. Redundancies, development and the flow of information. *BioEssays* **14**, 263–266 (1992).
19. Garrec, J. F. et al. A predictive model of asymmetric morphogenesis from 3D reconstructions of mouse heart looping dynamics. *eLife* **6**, e28951 (2017).

nature research

Corresponding author(s):   M Angela Nieto

Last updated by author(s): June 26, 2020

Reporting Summary

Nature Research wishes to improve the reproducibility of the work that we publish. This form provides structure for consistency and transparency in reporting. For further information on Nature Research policies, see Authors & Referees and the Editorial Policy Checklist.

Statistics

For all statistical analyses, confirm that the following items are present in the figure legend, table legend, main text, or Methods section.

n/a	Confirmed	
☐	☒	The exact sample size (n) for each experimental group/condition, given as a discrete number and unit of measurement
☐	☒	A statement on whether measurements were taken from distinct samples or whether the same sample was measured repeatedly
☐	☒	The statistical test(s) used AND whether they are one- or two-sided *Only common tests should be described solely by name; describe more complex techniques in the Methods section.*
☒	☐	A description of all covariates tested
☒	☐	A description of any assumptions or corrections, such as tests of normality and adjustment for multiple comparisons
☐	☒	A full description of the statistical parameters including central tendency (e.g. means) or other basic estimates (e.g. regression coefficient) AND variation (e.g. standard deviation) or associated estimates of uncertainty (e.g. confidence intervals)
☐	☒	For null hypothesis testing, the test statistic (e.g. F, t, r) with confidence intervals, effect sizes, degrees of freedom and P value noted *Give P values as exact values whenever suitable.*
☒	☐	For Bayesian analysis, information on the choice of priors and Markov chain Monte Carlo settings
☒	☐	For hierarchical and complex designs, identification of the appropriate level for tests and full reporting of outcomes
☒	☐	Estimates of effect sizes (e.g. Cohen's d, Pearson's r), indicating how they were calculated

Our web collection on statistics for biologists contains articles on many of the points above.

Software and code

Policy information about availability of computer code

Data collection	The software used to collect data includes: ImageJ 1.52p with Java 1.8.0_66, Leica Application Suite Software LAS V4.6.2, Zeiss ZEN Microscope Software ZEN Black 9.2.8.5, Olympus FV-ASW 4.2, DNastar Lasergene 15.0
Data analysis	Data analysis was performed with Microsoft Excel 2016, GraphPad Prism 7. Images were prepared using Adobe Photoshop and Adobe Illustrator from CS6.

For manuscripts utilizing custom algorithms or software that are central to the research but not yet described in published literature, software must be made available to editors/reviewers. We strongly encourage code deposition in a community repository (e.g. GitHub). See the Nature Research guidelines for submitting code & software for further information.

Data

Policy information about availability of data

All manuscripts must include a data availability statement. This statement should provide the following information, where applicable:

- Accession codes, unique identifiers, or web links for publicly available datasets
- A list of figures that have associated raw data
- A description of any restrictions on data availability

All data generated and analysed during this study are included in this published article and its supplementary information files.

Field-specific reporting

Please select the one below that is the best fit for your research. If you are not sure, read the appropriate sections before making your selection.

☒ Life sciences ☐ Behavioural & social sciences ☐ Ecological, evolutionary & environmental sciences

Life sciences study design

All studies must disclose on these points even when the disclosure is negative.

Sample size	For CRISPR injected embryos in each experiment a group of at least 100 embryos were injected with the corresponding reagents in a plate. After developing to the appropriate stage alive embryos without gross morphological defects were used for subsequent experiments. Fig 1b, 1c, 1f, 1g and 2b.
	For expression analyses via ISH at least 10 embryos per condition were analyzed. Detail as follows:
	For spaw, myl7, prrx1a, snail1b and twist1a expression embryos were hybridized in groups of 30. Fig 1c, 1f, 1g and 2b.
	For amhc immunodetection groups of 10 embryos were analyzed Fig 1d
	For prrx1 immunodetection a group of 10 embryos of each condition was used Fig 1b
	For a-tubulin detection groups of 10 embryos were analyzed Fig 1e
	We did not performed a prehoc test to determine sample size. The sample size for the injection experiments was chosen to be 100 the minimum to have enough surviving embryos to analyse. In most cases the sample size was larger than the minimum.
	For in situ hybridizations 30 embryos per group were chosen since this is the size that can be handled properly following our SEP. Immunodetections: we have chosen 10 to prevent antibody dilution due to the volume of the samples.
	In the hybridization and immunodetection experiments we defined the experiment successful only if at least a 80% of the embryos showed the same pattern.
Data exclusions	After injection with CRISPR components embryos that were dead or had stopped their development were excluded
	After immunodetection or in situ hybridization samples that were damaged, showed no expression or high background were excluded from the analysis
Replication	All replication attempts of the experiments were successful. Al experiments were repeated at least twice in different days using the same experimental procedures. In the injection experiments there was always a set of embryos from the same clutch that was kept in similar incubation conditions. Experiments were discarded when the control embryos showed malformations.
	Duplicates were analysed for differences from the other replicates, we did nor detect any differences between replicates.
Randomization	All animals were randomly selected for experiments.
Blinding	Blinding was not possible since in most cases it was possible to identify which sample was being scored. To prevent biases, at least two individuals checked the analysis of experiments. We defined a scoring system for heart position that was applied to every experiment. See Rago et al 2019 Dev Cell for details

Reporting for specific materials, systems and methods

We require information from authors about some types of materials, experimental systems and methods used in many studies. Here, indicate whether each material, system or method listed is relevant to your study. If you are not sure if a list item applies to your research, read the appropriate section before selecting a response.

Materials & experimental systems

n/a	Involved in the study
☐	☒ Antibodies
☒	☐ Eukaryotic cell lines
☒	☐ Palaeontology
☐	☒ Animals and other organisms
☒	☐ Human research participants
☒	☐ Clinical data

Methods

n/a	Involved in the study
☒	☐ ChIP-seq
☒	☐ Flow cytometry
☒	☐ MRI-based neuroimaging

Antibodies

Antibodies used	Rabbit anti Prrx1 (for IF). Tanaka lab. Used at 1:200
	Alexa Fluor 488 goat anti-rabbit. Invitrogen. A11008. Used at 1:500
	Mouse anti-aetylated alpha-tubulin. Sigma. T6793. Used at 1:600
	Alexa Fluor 568 goat anti-mouse Invitrogen. A11004. Used at 1:500
	Chicken IgY anti- GFP. Aveslab (2BScientific), GFP-1020. Used at 1:500
	Alexa Fluor 488 goat anti-chicken IgG (H+L). Life Technologies, A11039).Used at 1:500
	DIG-AP Fab fragments: sheep polyclonal. Roche (11093274910) Used at 1:500
Validation	Rabbit anti Prrx1 has been validated for zebrafish in Ocana et al. 2017, Nature.
	Mouse anti-acetylated alpha-tubulin. Sigma T6793. Specificity is described in the Sigma web page and it was tested in our lab in control zebrafish AB embryos.
	Chicken IgY anti- GFP Aveslab (2BScientific), GFP-1020 specificity is described by the manufacturer and was tested in our lab by

comparing GFP positive zebrafish embryos with AB wt embryos.
DIG-AP Fab fragments: sheep polyclonal, Roche (11093274910) specificity is described by the manufacturer and was tested in our lab by comparing reactivity of the antibody in zebrafish embryos that were hybridized without a labeled probe.

Animals and other organisms

Policy information about studies involving animals; ARRIVE guidelines recommended for reporting animal research

Laboratory animals	Fertilized eggs from zebrafish strain AB were used. All zebrafish embryos were between 0 and 60 hours post fertilization.
Wild animals	No wild animals were used
Field-collected samples	No Field-collected samples were used
Ethics oversight	The protocols were approved by the Spanish National Research Council (CSIC) Ethical Committee and the Animal Welfare Committee at the Institute of Neurosciences, Alicante.

Note that full information on the approval of the study protocol must also be provided in the manuscript.